

Dependence of Perpendicular Viscosity on Magnetic Fluctuations in a Stochastic TopologyR. Fridström,¹ B. E. Chapman,² A. F. Almagri,² L. Frassinetti,¹ P. R. Brunzell,¹ T. Nishizawa,² and J. S. Sarff²¹*Department of Fusion Plasma Physics, School of Electrical Engineering,
KTH Royal Institute of Technology, SE-10044 Stockholm, Sweden*²*Department of Physics, University of Wisconsin–Madison, 1150 University Avenue, Madison, Wisconsin 53706, USA* (Received 5 December 2017; revised manuscript received 21 March 2018; published 30 May 2018)

In a magnetically confined plasma with a stochastic magnetic field, the dependence of the perpendicular viscosity on the magnetic fluctuation amplitude is measured for the first time. With a controlled, \sim tenfold variation in the fluctuation amplitude, the viscosity increases \sim 100-fold, exhibiting the same fluctuation-amplitude-squared dependence as the predicted rate of stochastic field line diffusion. The absolute value of the viscosity is well predicted by a model based on momentum transport in a stochastic field, the first in-depth test of this model.

DOI: [10.1103/PhysRevLett.120.225002](https://doi.org/10.1103/PhysRevLett.120.225002)

Viscosity characterizes the rate of momentum transport within a fluid and plays an important role in fluid stability. The viscosity can be expressed in terms of its dynamic or absolute value but also in terms of its kinematic value, normalizing the dynamic viscosity to the mass density. For a two-fluid plasma consisting of electrons and ions, momentum is carried primarily by the ions, and viscosity affects the rate of ion momentum transport. If the plasma is embedded in a magnetic field, the viscosity is anisotropic. The viscosity in the direction parallel to the field is the same as that for an unmagnetized plasma, but perpendicular to the field the viscosity and momentum transport are reduced.

The classical lower bound on perpendicular or cross-field viscosity in a magnetized plasma was derived by Braginskii [1] for the case of viscosity dominated by ion-ion collisions. The Braginskii viscosity has been *assumed* to apply in many astrophysical and laboratory plasmas, e.g., the flaring solar corona [2], clusters of galaxies [3], and the tokamak fusion plasma [4]. But measurements confirming the relevance of the Braginskii viscosity have been rare. One exception was in a few-eV screw-pinch plasma column where the ion viscosity agreed with the Braginskii value to within a factor of 2 [5].

Measurements of the perpendicular viscosity have also been made in the reversed-field pinch (RFP) plasma [6,7], a high-temperature toroidal magnetic fusion configuration that can exist in a steady fashion with a stochastic magnetic topology, where field lines wander chaotically, over much of the plasma volume. The measured viscosity was as much as 100 times the Braginskii value. Stochastic magnetic topologies can also occur in other configurations such as the tokamak, stellarator, and spheromak, e.g., Refs. [8–10]. Stochasticity in the tokamak, for example, occurs locally in the plasma edge when applying an external magnetic perturbation [11] and globally during disruptions [12],

wherein magnetohydrodynamic (MHD) instabilities lead to the premature termination of the discharge [13].

In astrophysical plasmas, viscous momentum transport in stochastic magnetic fields occurs, for example, in accretion disks [14,15]. Another astrophysical phenomenon where viscosity and stochastic magnetic fields may play a role is when a so-called cold front propagates into a magnetized medium [16,17].

Nonlinear viscoresistive MHD computation is used for both astrophysical and laboratory plasmas to model scenarios with magnetic stochasticity, e.g., Refs. [14,18–21]. However, while the resistivity is sometimes provided by measurements, the viscosity must be assumed.

A model was proposed by Finn, Guzdar, and Chernikov [22] to describe the transport of momentum and particles in a stochastic field. Motivated to help explain the physics of the transition to the high-confinement mode in tokamaks, momentum in the model is transported along stochastic field lines by sound wave propagation. The kinematic viscosity is assumed to be proportional to the square of the magnetic fluctuation amplitude, utilizing the quasilinear stochastic magnetic diffusion coefficient derived by Rosenbluth *et al.* [23]. While the magnetic diffusion coefficient has been tested in the context of electron heat transport in both astrophysical [24,25] and laboratory [26,27] plasmas, there has been no in-depth test of the Finn model for momentum transport. In their paper, Finn, Guzdar, and Chernikov suggest that their model could be tested in a tokamak in which internal magnetic fluctuations are varied via an external magnetic perturbation.

In this Letter, we adopt an alternative approach, comparing measured and modeled viscosities in stochastic RFP plasmas, wherein the amplitude of the underlying magnetic fluctuations is varied both through magnetic self-organization and through external inductive control. The fluctuations arise due to tearing modes (TMs) driven

unstable by the gradient in the plasma current. The viscosity is measured experimentally via perturbations to the momentum profile: acceleration with an insertable biased probe [6] and deceleration with a resonant magnetic perturbation (RMP) [28,29]. We thereby show that (i) with a \sim tenfold variation in fluctuation amplitude, the viscosity varies \sim 100-fold, exhibiting the same fluctuation-amplitude-squared dependence as the predicted rate of stochastic field line diffusion, and (ii) the absolute value of the viscosity is well predicted by the Finn model.

Experimental data were gathered in the Madison Symmetric Torus (MST) [30] RFP. This toroidal device has major and minor radii of $R = 1.5$ m and $a = 0.52$ m. Deuterium (D) plasmas were Ohmically heated with a toroidal plasma current ranging from 50 to 400 kA. The line-averaged electron density was varied from 0.3 to 1.5×10^{19} m $^{-3}$. The TM amplitudes and phase velocities were measured by magnetic pick-up coils at the plasma boundary. The dominant TMs have poloidal mode number $m = 1$ with different toroidal mode numbers n . These modes corotate with the plasma [6,31], resembling the large TM amplitude case in the tokamak [32]. Each mode is resonant where the safety factor $q \equiv (rB_\phi)/(RB_\theta) = m/n$, where B_ϕ and B_θ are the equilibrium toroidal and poloidal fields. At each resonant surface, a magnetic island forms, and island overlap leads to stochasticity. The degree of overlap increases with the amplitudes of neighboring TMs. The amplitude of each TM at its resonant surface is calculated from the radial eigenfunction [29].

Three different magnetic equilibria were employed in this work, characterized by the edge safety factor: $q(a) = 0$, -0.07 , and a time-varying equilibrium with $q(a)_{\min} = -0.2$. In the $q(a) = 0$ plasmas, the fluctuation level decreases through self-organization with an increasing plasma current, and the $q(a) = -0.07$ plasmas exhibit an additional spontaneous reduction in the fluctuation level [33]. In the $q(a)_{\min} = -0.2$ case, the fluctuations are still further reduced by the application of inductive modification of the current profile [34,35].

The classical width of a magnetic island $w_{mn} = 4\sqrt{r_{mn}|b_{r,mn}|/(nB_\theta|q'_{mn}|)}$, where $b_{r,mn}$ is the radial component of the tearing magnetic fluctuation, q'_{mn} is a radial derivative, and all quantities are defined at the resonant surface, minor radius r_{mn} . The degree of overlap between two islands, (m, n) and (m', n') , can be quantified by the Chirikov parameter s [36]. Island overlap ($s > 1$) causes the field lines to become entangled, and the radial excursion Δr over a distance L along a field line can be described by a stochastic process. Averaging over several steps, the diffusion coefficient for a magnetic field line is

$$D_{\text{mag}} = \langle \Delta r^2 \rangle / 2L. \quad (1)$$

In a collisionless plasma, transport can occur directly along a single field line over the whole stochastic region. In

the MST plasmas described here, the collisionless regime [22,37] is a reasonable approximation, since the range of the ion mean free path (1–30 m) is at a minimum similar to the autocorrelation length [38] $L_c \approx 1$ m [39].

The diffusion of electrons in a stochastic magnetic field was described by Rechester and Rosenbluth (RR) [37], who posited that the heat diffusivity in the collisionless limit, $\chi_e = v_e D_{\text{mag}R}$, where v_e is the electron thermal velocity and

$$D_{\text{mag}R} = L_c \sum_{m,n} \left(\frac{b_{r,mn}}{B} \right)^2 \quad (2)$$

is the magnetic diffusion coefficient in the quasilinear approximation [23]. Here, B is defined at r_{mn} . The TMs that overlap are included in the sum, which we shall henceforth denote simply as $(b/B)^2$. The RR model assumes $s \gg 1$.

Finn, Guzdar, and Chernikov [22] assumed a similar model for the transport of momentum, but the transport occurs due to sound wave propagation. Accordingly, the kinematic viscosity in a stochastic field is

$$\nu_{\perp,st} = c_s D_{\text{mag}R}. \quad (3)$$

We calculate the sound speed c_s using

$$c_s = \sqrt{(\gamma_e Z k_B T_e + \gamma_i k_B T_i) / M}. \quad (4)$$

The electron temperature T_e was measured with a Thomson scattering diagnostic [40]. The ion temperature T_i was inferred from earlier spectroscopic measurements in similar MST plasmas [41]. We assume a pure D plasma with isothermal electrons ($\gamma_e = 1$) and one degree of freedom for the ions ($\gamma_i = 3$). Because of impurities, the effective charge and mass are moderately higher than for a pure D plasma, but the impact is muted given the dependence of Z and M in the sound speed.

To calculate $D_{\text{mag}R}$ [Eq. (2)], we require the values of L_c and b/B . The autocorrelation length was calculated using the model in Ref. [38], which had agreement with numerical calculations for the RFP [42]. We estimate $L_c = \pi / \Delta k_{\parallel} \approx 1.2 \pm 0.4$ m, for all scenarios. The parallel spectral width $\Delta k_{\parallel} = (\Delta m/a)(B_\theta/B) + (\Delta n/R)(B_\phi/B)$, where poloidal mode spectrum width $\Delta m = 0.5$ had the best agreement with magnetic probe measurements, and the toroidal width is $\Delta n \approx 4$ [39]. In the calculation of b/B , we used the time-averaged rms amplitude of the three innermost TMs whose islands overlap. The inclusion of additional TMs, which are of lower amplitude, has only a small effect on $D_{\text{mag}R}$. We calculated the 1σ error in $\nu_{\perp,st}$ by propagating uncertainties through Eqs. (2)–(4). We note that neither the probe nor the RMP affect the measured mode spectrum, and therefore $D_{\text{mag}R}$ is also unaffected. This is in contrast to the tokamak, where RMPs can destabilize additional TMs [43], and biased probes either suppress or destabilize the TMs [44].

Experimentally, we determined the viscosity by modeling the radial transport of the perturbed momentum. The transport was modeled by solving the toroidal component of the momentum equation

$$\rho \frac{\partial \Delta v_\phi}{\partial t} = \frac{1}{r} \frac{\partial}{\partial r} \left(r \mu_\perp \frac{\partial \Delta v_\phi}{\partial r} \right) + T_{\text{injected}}, \quad (5)$$

where the injected torque density (T_{injected}) is from either the probe or the RMP, ρ is the mass density, Δv_ϕ is the perturbed radial profile of the toroidal plasma flow, and $\mu_\perp(r)$ is the perpendicular dynamic viscosity. The dynamic viscosity is assumed to be spatially constant, $\mu_\perp = \rho_0 \nu_\perp$, where the central mass density ρ_0 is determined from the measurement. The electron density profile, measured with a multichord interferometer [45], is well approximated by $n_e = n_{e0}[1 - (r/a)^3]$. The deuteron density is assumed equal to the electron density. The kinematic viscosity (ν_\perp) is the only free parameter in the model, and its value is chosen to match the experimental momentum transport. A flat viscosity profile is suggested as a good approximation by the fact that the D_{mag} profile is typically flat in the core [26,46], as are the temperature and density profiles. And the fit viscosity is most sensitive to the value in the core [29]. Hence, the fit value represents approximately the core average.

The plasma response to the biased probe [6] is shown in Fig. 1, from an ensemble average of 20 shots with $q(a) = 0$, $I_\phi = 200$ kA, and $\langle n_e \rangle \approx 0.7 \times 10^{19} \text{ m}^{-3}$. Inserted to $r/a \approx 0.8$, the probe is biased for 10 ms to ~ 0.4 kV relative to the MST vacuum vessel, resulting in a drawn current of ~ 1 kA [Fig. 1(a)] and a $\mathbf{J} \times \mathbf{B}$ torque imposed on the edge plasma. The toroidal flow in the edge [Fig. 1(b)], inferred from the Doppler shift of the CIII impurity emission, responds quickly to the bias and saturates. The core flow, represented by the velocity of the innermost resonant (1,5) TM, increases slowly throughout the bias period [Fig. 1(c)]. After the biasing, the edge once again responds more promptly than the core.

The slowing-down timescale of the core flow, τ_{sd} , is inversely proportional to the viscosity [6], $\nu_\perp = d^2/\tau_{\text{sd}}$, where d is the radial extent over which momentum diffuses. The best fit of the deceleration curve to the function $v_\phi = A \exp(-t/\tau_{\text{sd}}) + v_0$ has $\tau_{\text{sd}} = 3.3$ ms. This is about 1.3 times longer than that measured previously in MST hydrogen (H) plasmas with a similar equilibrium [6]. Assuming that d and $D_{\text{mag}R}$ are the same with H and D, Eq. (3) predicts the ratio of the slowing-down times to be $\tau_{\text{sd}D}/\tau_{\text{sd}H} = c_{sH}/c_{sD} \approx 1.3$, suggesting that the difference in τ_{sd} could be due to the difference in the plasma sound speed.

The radial transport of momentum during bias is depicted by the change in the velocity of TMs resonant at different radii [Fig. 1(d)]. Initially, the CIII ions and the TMs closest to the probe are accelerated. Later, all the

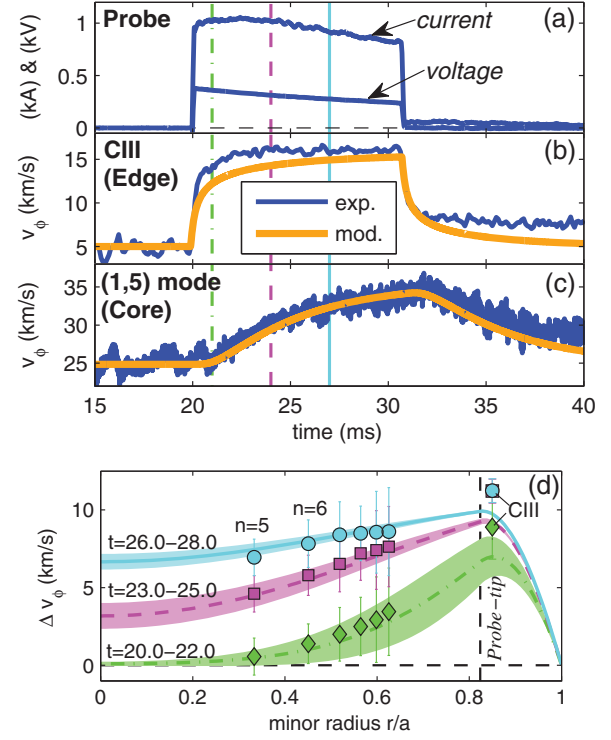


FIG. 1. (a) Probe bias voltage and current, (b) CIII toroidal flow and modeled plasma flow at $r/a = 0.81$, (c) toroidal phase velocity of central (1,5) TM and modeled plasma flow at the (1,5) resonant surface, (d) measured (data points) and modeled perturbed velocity profile at three time intervals, the centers of which are indicated by vertical lines in (a)–(c). Experimental profiles in (d) are based on the change in rotation of the $n = 5-10$ modes. Modeled profiles represent the change in plasma flow. The 1σ error bars represent the change in each time window. The phase velocities of the core modes ($n = 5-10$) are used to constrain the modeled $\Delta v_\phi(r)$, whereas the CIII velocity is shown only as a visual test of the modeling of the edge.

core TMs have been accelerated through the viscous transfer of momentum.

The transport depicted in Fig. 1 was modeled with Eq. (5). The torque density produced by the probe during the bias is assumed to fall off as $1/r$ from the probe tip to the plasma boundary. This was motivated by the fact that the current density decreases as $1/r$ and that the magnetic field changes only slightly ($\pm 5\%$) in this region. This torque was adjusted such that the modeled and experimental velocity profiles match at the end of the biasing period. After biasing, ν_\perp is the only free parameter in the model, and by matching the experimental core deceleration curve [Fig. 1(c)] it was found that $\nu_\perp = 15 \pm 5 \text{ m}^2/\text{s}$. The uncertainty includes the change in ν_\perp when the modeled plasma density is varied within the experimental 1σ standard deviation. Using probe bias, we measured ν_\perp in $q(a) = 0$ plasmas at three plasma currents (Table I). The viscosity increases from 15 ± 5 to $55 \pm 12 \text{ m}^2/\text{s}$ as I_ϕ drops from 200 to 49 kA. We show below that this can be

TABLE I. Experimental and model viscosities for different plasma conditions. The Chirikov parameter (s) was calculated for two innermost TMs included in $D_{\text{mag}R}$. Errors are 1σ standard deviation.

Method	$q(a)$	I_ϕ (kA)	c_s (km/s)	b/B (%)	s	$\nu_{\perp,\text{exp}}$ (m ² /s)	$\nu_{\perp,\text{st}}$ (m ² /s)	$\nu_{\perp,\text{Brag}}$ (m ² /s)
Probe	0	49	90	2.3	3.5	55 ± 12	56 ± 20	3.93 ± 1.06
RMP	0	125	160	1.3	2.3	30 ± 9	30 ± 5	0.34 ± 0.11
Probe	0	124	160	1.2	2.3	30 ± 8	28 ± 10	0.40 ± 0.11
Probe	0	200	200	1.0	2.2	15 ± 5	25 ± 10	0.14 ± 0.04
RMP	0	208	190	1.0	2.2	21 ± 6	24 ± 5	0.18 ± 0.06
RMP	0	302	220	0.9	2.0	20 ± 5	24 ± 5	0.09 ± 0.02
RMP	0	396	250	0.8	1.9	17 ± 6	19 ± 5	0.05 ± 0.01
RMP	-0.07	338	260	0.6	1.6	10 ± 3	13 ± 2	0.04 ± 0.00
RMP	-0.2	182	210	0.2	1.2	0.6 ± 0.3	1.1 ± 0.7	0.14 ± 0.03

explained by the self-organized increase in b/B as I_ϕ decreases.

Complementing the biasing technique, we utilized braking with the RMP technique [29,47], in which an external $m = 1$ RMP produces an electromagnetic torque at each TM resonant surface [48]. Injected through a cut in MST's conducting shell, this torque acts to reduce the phase difference between the rotating TMs and the static RMP. Utilization of the RMP expands the parameter space accessible for this work to higher-energy-density plasmas that would damage the inserted biased probe. And applying the RMP and biased probe to the same set of plasma conditions provides a valuable cross-check on the measured viscosity.

In Fig. 2 are waveforms from a single discharge with an RMP. The plasma parameters [$q(a) = 0$, $I_\phi = 200$ kA, and $\langle n_e \rangle \approx 1.0 \times 10^{19} \text{ m}^{-3}$] were similar to those for the data in Fig. 1, but with a higher density. With the application of the RMP, the core rotation velocity, represented here by the velocity of the two innermost resonant $m = 1$ TMs, gradually slows and finally drops to zero. The TM velocities and plasma flow were modeled by solving the momentum equation [Eq. (5)], as described in Ref. [29]. Similar to the biased-probe modeling, the only free parameter here is the viscosity, and it is estimated by matching the experimental deceleration

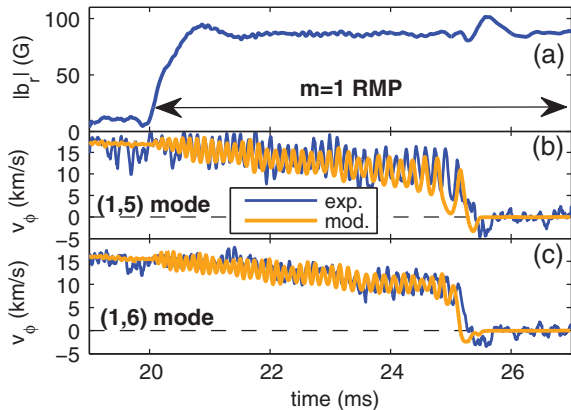


FIG. 2. (a) Applied $m = 1$ RMP amplitude and (b), (c) toroidal phase velocities of (1,5) and (1,6) TMs.

of the TMs. Figures 2(b) and 2(c) show, for example, the model fit to the experimental velocity of the two largest TMs.

Averaging over ten similar discharges like that in Fig. 2, the model-required viscosity is $\nu_{\perp} = 21 \pm 6 \text{ m}^2/\text{s}$, where the uncertainty is the 1σ standard deviation including both the uncertainty in the model input and the shot-to-shot deviation in the viscosity. This value, within the uncertainty, is consistent with the value measured using the biased probe in similar plasma conditions. In the same fashion, the RMP was used to measure the viscosity in five additional plasma conditions, each with a different b/B . The results are listed in Table I, showing that ν_{\perp} generally increases with b/B . The table also shows that, at $I_\phi \approx 125$ kA, the values of ν_{\perp} measured with the RMP and probe are identical.

All of the probe and RMP measurements of viscosity are compared in Fig. 3 with the models of Rosenbluth *et al.* and Finn, Guzdar, and Chernikov. The dependence of the viscosity on (b/B) is shown in Fig. 3(a), where the measured viscosity is divided by the plasma sound speed

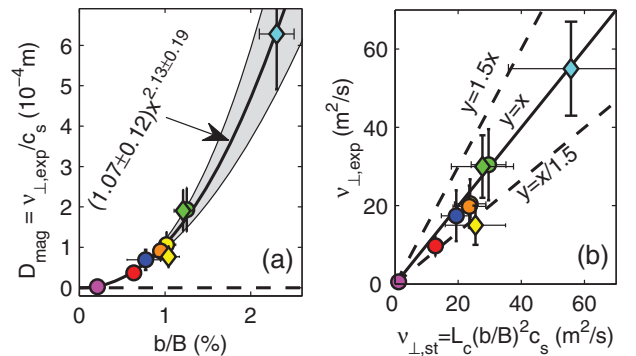


FIG. 3. For the RMP (circles) and probe (diamonds) cases, (a) the measured viscosity divided by the plasma sound speed versus the normalized magnetic fluctuation amplitude and (b) the measured viscosities versus predictions by Eq. (3). In (a), the best fit of function $y = Cx^a$ is a solid line with the uncertainty estimate indicated by a gray area. Different symbol color is used for each plasma scenario: $q(a)_{\text{min}} = -0.2$ current profile control (magenta), $q(a) = -0.07$ (red), and $q(a) = 0$ at 400 (blue), 300 (orange), 200 (yellow), 125 (green), and 50 kA (cyan).

(Table I). The best fit to the experimental data, $D_{\text{mag}} = (1.07 \pm 0.12)(b/B)^{2.13 \pm 0.19}$, is in good agreement with the expectation $(b/B)^2$ for the quasilinear stochastic magnetic diffusion coefficient [Eq. (2)]. And as shown in Table I, (b/B) spans \sim tenfold, while the experimental viscosity spans \sim 100-fold. In Fig. 3(b), the measured viscosities are compared directly to the predictions, $\nu_{\perp, st}$, of the Finn model. Within the estimated uncertainties, shown numerically in Table I, the viscosities agree in all cases, consistent with the magnetic fluctuations and stochasticity being responsible for the anomalous transport of momentum. This is also consistent with a previous estimate in stochastic hydrogen MST plasmas [6], where a single measured viscosity agreed reasonably well with the Finn model.

In modeling the momentum transport [Eq. (5)], the intrinsic momentum source was not included, but this would affect our conclusions only if the probe or RMP changes the source. The likely source is the fluctuation-based kinetic stress [49], and (i) neither perturbative technique has much effect on the fluctuation amplitudes, and (ii) the viscosity measured with the two techniques is about the same, even though their impact, if any, on the kinetic stress might be expected to differ.

As expected, the experimental viscosities are all larger than the classical predictions, $\nu_{\perp, \text{Brag}} = 3n_i T_i / (10\omega_i^2 \tau_i)$, where ω_i and τ_i are the ion Larmor frequency and collision time, respectively [1]. It is, however, interesting that the viscosity in the case with the lowest fluctuation amplitude is within a factor of 4 of $\nu_{\perp, \text{Brag}}$ (Table I), suggesting that this case is near the limit of the domain where a stochastic field can be assumed. This is consistent with the near-threshold island overlap criterion ($s = 1.2$) and the fact that the stochastic prediction for the viscosity is nearly twice the experimental value (Table I).

In summary, our results confirm for the first time that the kinematic viscosity in a stochastic magnetic topology can be modeled by momentum propagated by sound waves along the magnetic field lines. This work is applicable to tokamak, stellarator, RFP, and other laboratory plasmas, along with a variety of astrophysical plasmas, in which magnetic stochasticity plays an important role. Viscous resistive MHD modeling of these plasmas can now be better constrained and should therefore be more realistic, contributing further to the predictive capability of the science of high-temperature, magnetically confined plasmas.

Data shown in this Letter can be obtained in Supplemental Material Ref. [50].

We thank J. M. Finn for helpful theoretical discussions and J. Boguski, P. J. Fimognari, C. M. Jacobson, K. J. McCollam, and the entire MST team for help with gathering and analyzing data. We thank E. G. Zweibel for help in connecting our work to astrophysical plasmas. This material is based upon work supported by the U.S. Department of Energy Office of Science, Office of Fusion Energy Sciences program under Award No. DE-FC02-05ER54814.

- [1] S. I. Braginskii, *Rev. Plasma Phys.* **1**, 205 (1965).
- [2] I. Craig and Y. Litvinenko, *Astron. Astrophys.* **501**, 755 (2009).
- [3] A. A. Schekochihin, S. C. Cowley, R. M. Kulsrud, G. W. Hammett, and P. Sharma, *Astrophys. J.* **629**, 139 (2005).
- [4] V. A. Rozhansky, S. P. Voskoboinikov, E. G. Kaveeva, D. P. Coster, and R. Schneider, *Nucl. Fusion* **41**, 387 (2001).
- [5] L. Dorf, T. Intrator, X. Sun, J. Hendryx, G. Wurden, I. Furno, and G. Lapenta, *Phys. Plasmas* **17**, 102101 (2010).
- [6] A. F. Almagri, J. T. Chapman, C. S. Chiang, D. Craig, D. J. Den Hartog, C. C. Hegna, and S. C. Prager, *Phys. Plasmas* **5**, 3982 (1998).
- [7] L. Frassinetti, K. E. J. Olofsson, P. R. Brunzell, and J. R. Drake, *Nucl. Fusion* **50**, 035005 (2010).
- [8] O. Dumbrajs *et al.*, *Nucl. Fusion* **48**, 024011 (2008).
- [9] H. Himura, H. Wakabayashi, M. Fukao, Z. Yoshida, M. Isobe, S. Okamura, C. Suzuki, S. Nishimura, K. Matsuoka, K. Toi, and H. Yamada, *Phys. Plasmas* **11**, 492 (2004).
- [10] H. S. McLean, R. D. Wood, B. I. Cohen, E. B. Hooper, D. N. Hill, J. M. Moller, C. Romero-Talamas, and S. Woodruff, *Phys. Plasmas* **13**, 056105 (2006).
- [11] T. E. Evans *et al.*, *Phys. Rev. Lett.* **92**, 235003 (2004).
- [12] V. Igochine *et al.*, *Nucl. Fusion* **46**, 741 (2006).
- [13] F. C. Schuller, *Plasma Phys. Controlled Fusion* **37**, A135 (1995).
- [14] R. Matsumoto and T. Tajima, *Astrophys. J.* **445**, 767 (1995).
- [15] K. Shirakawa and M. Hoshino, *Phys. Plasmas* **21**, 052903 (2014).
- [16] L. Dursi and C. Pfrommer, *Astrophys. J.* **677**, 993 (2008).
- [17] N. Asai, N. Fukuda, and R. Matsumoto, *Astrophys. J.* **663**, 816 (2007).
- [18] D. Bonfiglio, M. Veranda, S. Cappello, D. F. Escande, and L. Chacón, *Phys. Rev. Lett.* **111**, 085002 (2013).
- [19] R. Paccagnella, H. R. Strauss, and J. Breslau, *Nucl. Fusion* **49**, 035003 (2009).
- [20] M. T. Beidler, C. C. Hegna, C. R. Sovinec, J. D. Callen, and N. M. Ferraro, in *APS Meeting Abstracts* (American Physical Society, New York, 2016).
- [21] D. Bonfiglio, M. Veranda, S. Cappello, L. Chacón, and D. F. Escande, *Plasma Phys. Controlled Fusion* **59**, 014032 (2017).
- [22] J. M. Finn, P. N. Guzdar, and A. A. Chernikov, *Phys. Fluids B* **4**, 1152 (1992).
- [23] M. N. Rosenbluth, R. Z. Sagdeev, J. B. Taylor, and G. M. Zaslavski, *Nucl. Fusion* **6**, 297 (1966).
- [24] B. D. G. Chandran and S. C. Cowley, *Phys. Rev. Lett.* **80**, 3077 (1998).
- [25] A. Baldi, W. Forman, C. Jones, P. Nulsen, L. David, R. Kraft, and A. Simionescu, *Astrophys. J.* **694**, 479 (2009).
- [26] T. M. Biewer *et al.*, *Phys. Rev. Lett.* **91**, 045004 (2003).
- [27] J. A. Reusch, J. K. Anderson, D. J. Den Hartog, F. Ebrahimi, D. D. Schnack, H. D. Stephens, and C. B. Forest, *Phys. Rev. Lett.* **107**, 155002 (2011).
- [28] S. Munaretto, B. E. Chapman, D. J. Holly, M. D. Nornberg, R. J. Norval, D. J. Den Hartog, J. A. Goetz, and K. J. McCollam, *Plasma Phys. Controlled Fusion* **57**, 104004 (2015).
- [29] R. Fridström, S. Munaretto, L. Frassinetti, B. E. Chapman, P. R. Brunzell, and J. S. Sarff, *Phys. Plasmas* **23**, 062504 (2016).

- [30] R. Dexter, D. Kerst, T. Lovell, S. Prager, and J. Sprott, *Fusion Technol.* **19**, 131 (1991).
- [31] B. E. Chapman, R. Fitzpatrick, D. Craig, P. Martin, and G. Spizzo, *Phys. Plasmas* **11**, 2156 (2004).
- [32] G. Ronchi, J. Severo, F. Salzedas, R. Galvão, and E. Sanada, *Plasma Phys. Rep.* **42**, 465 (2016).
- [33] B. E. Chapman, C.-S. Chiang, S. C. Prager, J. S. Sarff, and M. R. Stoneking, *Phys. Rev. Lett.* **80**, 2137 (1998).
- [34] J. S. Sarff, S. A. Hokin, H. Ji, S. C. Prager, and C. R. Sovinec, *Phys. Rev. Lett.* **72**, 3670 (1994).
- [35] B. E. Chapman *et al.*, *Phys. Plasmas* **9**, 2061 (2002).
- [36] B. V. Chirikov, *Phys. Rep.* **52**, 263 (1979).
- [37] A. B. Rechester and M. N. Rosenbluth, *Phys. Rev. Lett.* **40**, 38 (1978).
- [38] J. A. Krommes, C. Oberman, and R. G. Kleva, *J. Plasma Phys.* **30**, 11 (1983).
- [39] M. R. Stoneking, Ph.D. thesis, University of Wisconsin-Madison, 1994.
- [40] D. J. D. Hartog, J. R. Ambuel, M. T. Borchardt, A. F. Falkowski, W. S. Harris, D. J. Holly, E. Parke, J. A. Reusch, P. E. Robl, H. D. Stephens, and Y. M. Yang, *Rev. Sci. Instrum.* **81**, 10D513 (2010).
- [41] B. E. Chapman *et al.*, *Phys. Rev. Lett.* **87**, 205001 (2001).
- [42] F. D'Angelo and R. Paccagnella, *Phys. Plasmas* **3**, 2353 (1996).
- [43] R. Buttery, M. De'Benedetti, T. Hender, and B. Tubbing, *Nucl. Fusion* **40**, 807 (2000).
- [44] I. Nascimento *et al.*, *Nucl. Fusion* **47**, 1570 (2007).
- [45] B. H. Deng, D. L. Brower, W. X. Ding, M. D. Wyman, B. E. Chapman, and J. S. Sarff, *Rev. Sci. Instrum.* **77**, 10F108 (2006).
- [46] B. Hudson, Ph.D. thesis, University of Wisconsin-Madison, 2006.
- [47] L. Frassinetti, S. Menmuir, K. E. J. Olofsson, P. R. Brunzell, and J. R. Drake, *Nucl. Fusion* **52**, 103014 (2012).
- [48] R. Fitzpatrick, E. Rossi, and E. P. Yu, *Phys. Plasmas* **8**, 4489 (2001).
- [49] W. X. Ding, L. Lin, D. L. Brower, A. F. Almagri, B. E. Chapman, G. Fiksel, D. J. Den Hartog, and J. S. Sarff, *Phys. Rev. Lett.* **110**, 065008 (2013).
- [50] See Supplemental Material <http://link.aps.org/supplemental/10.1103/PhysRevLett.120.225002> for Data shown in this Letter.